# Influence of Zirconia Nanofillers on Physical and Mechanical Characteristics of Palmyra Palm Fruit and Jackfruit Peel Fiber–Reinforced Polymer Composites

Nanthakumar *Sivasamy*[1], Kumaresan Govindasamy[2], Ananthi *Subramani*[3], Karthikeyan *Ravichandran*[4], Arunkumar *Singaravel*[5], and Girimurugan *Ramasamy*[6*]

[1]Department of Mechanical Engineering, PSG Institute of Technology and Applied Research, Coimbatore, Tamil Nadu, India
[2]Department of Mechanical Engineering, Bannari Amman Institute of Technology, Sathyamangalam, Tamil Nadu, India
[3]Department of Physics, Nandha College of Technology, Perundurai, Tamil Nadu, India
[4]Department of Automobile Engineering, Rajalakshmi Engineering College, Chennai, Tamil Nadu, India
[5]Department of Mechanical Engineering, Vinayaka Mission's Kirupananda Variyar Engineering College, Vinayaka Mission's Research Foundation (Deemed to be University), Salem, Tamil Nadu, India
[6]Department of Mechanical Engineering, Nandha College of Technology, Perundurai, Tamil Nadu, India

**Abstract.** This study seeks to examine the mechanical properties of epoxy composites reinforced with natural fibers derived from hybrid palmyra palm fruit waste and jackfruit (*Artocarpus heterophyllus*) peel waste fibers, as well as to evaluate the impact of varying zirconia ($ZrO_2$) nano filler loadings on their physical and mechanical attributes. A 5% NaOH solution was utilized to mercerize the fibers of the palmyra palm fruit, and X-ray diffraction (XRD) analysis verified the crystallinity of the treated fibers and $ZrO_2$ nanofillers. Three distinct loadings of $ZrO_2$ nano fillers (2.5 wt. %, 5 wt. %, and 7.5 wt. %) and three fiber fractions (20 wt. %, 25 wt. %, and 30 wt. %) were employed. Composites were manufactured via hand lay-up techniques, and evaluations were conducted in accordance with ASTM standards. The findings indicated that the incorporation of $nZrO_2$ markedly improved tensile strength (up to ~32 MPa), tensile modulus (up to ~1555 MPa), flexural strength (up to ~78 MPa), impact resistance (up to ~1.8 J), hardness (up to ~64 HV), and interlaminar shear strength (up to ~82 MPa) relative to unfilled composites, with optimal performance achieved at 25 wt. % fiber loading and moderate filler content (2.5–5 wt %). Excessive fiber or filler loadings (30 wt % fiber or ≥7.5 wt % filler) led to diminished characteristics due to agglomeration and an increase in voids (up to about 7 wt. %).

*Corresponding author: dr.r.girimurugan@gmail.com

Composites containing 5 wt. % $ZrO_2$ nanoparticles and 20 wt. % fiber (1:1 ratio of palmyra palm to jackfruit peel fiber) shown enhanced hardness, impact resistance, compressive strength, and flexural strength. Morphological investigation validated the effective interfacial bonding among $ZrO_2$ nanofillers, epoxy matrix and the natural fibers. The findings indicate that the produced composites possess promise for structural and non-structural applications under low to medium stress situations.

## 1 Introduction

Natural composites are sustainable materials created by integrating natural fibers with polymer, metal, or ceramic matrices to improve strength and durability. They are extensively investigated as sustainable substitutes for synthetic composites owing to their biodegradability, cost-effectiveness, and lightweight characteristics [1]. Glass, Kevlar, and carbon were once prevalent components of polymer composite materials; however, their utilization has diminished in recent years owing to significant environmental concerns. Cellulose extracted from jackfruit peel (28.04 % yield) was blended with PVA to develop biodegradable films. The 20 % cellulose–PVA composite showed best thermal stability (368.2°C) and mechanical properties, while higher loadings increased water absorption. The films are promising for eco-friendly packaging applications [2]. Jackfruit's natural impact-resistant structure was studied and mimicked using 3D printing. Its exterior and porous mesocarp delayed crack propagation, enhancing energy absorption. Bioinspired prints outperformed conventional ones in impact tests, showing potential for protective material design [3]. Microcrystalline cellulose (12.69 nm, CI 51.09 %) was extracted from *Terminalia catappa* leaves and incorporated into PLA biofilms. The 2 % TCLC-filled film reached 23.05 MPa tensile strength versus 20.65 MPa for neat PLA. Improved crystallinity and thermal stability suggest strong potential for food packaging [4]. Biodiesel was produced from *Borassus flabellifer* oil by transesterification and enhanced with ethanol and $Al_2O_3$ nanoparticles. The optimized blend (20BOPP+20E+60D+AONP) achieved BTE 31.94%, reduced NOx by 29.2%, CO by 11.4 %, and smoke by 35.3 % compared to diesel. The nano-fuel showed excellent performance in DICI engines [5]. Ultra-high molecular weight polyethylene composites reinforced with $ZrO_2$ nanoparticles were developed and evaluated for orthopedic applications. The nanocomposites showed enhanced compression modulus and wear resistance, particularly at 5–10 wt. % filler content. Taguchi analysis revealed that 5 wt.% $ZrO_2$ provided optimal wear reduction under simulated body fluid lubrication [6]. The PMMA nanocomposites reinforced with $ZrO_2$ and Ag nanoparticles were fabricated by casting. Mechanical tests revealed improved hardness and compression strength up to 2.25 wt. % filler loading. The results suggest potential use in dental applications due to improved structural performance [7]. Epoxy composites filled with zirconia-toughened alumina (ZTA) nanoparticles were prepared by ultrasonication. Mechanical tests showed maximum tensile, flexural, and compression strength at 1.5 wt. % ZTA loading. Electrical insulation performance was also enhanced, with 2.5 wt. % ZTA providing outstanding breakdown strength [8]. Licuala grandis leaf stalk fibers reinforced unsaturated polyester composites showed optimal strength at 30 wt. % with 5 mm fibers. Flexural (58 MPa), tensile (64.9 MPa), hardness (70.4 HRRW), and impact (5.4 J/cm²) values were obtained. SEM, FTIR, and XRD confirmed their suitability for automotive and aerospace interiors [9]. Natural fibers (jute, bamboo, flax) with different woven architectures in epoxy were evaluated. Jute–twill composites gave the highest tensile strength (91.83 MPa), while jute–basalt showed maximum flexural strength (212.25 MPa).

Flax–basalt composites were hydrophobic, whereas jute twill showed hydrophilic behavior [10]. Waste coconut and cactus fibers were reinforced with bentonite to develop eco-friendly acoustic composites. Tests showed improved hardness, reduced density, and stable acoustic coefficients under humidity and temperature. Coconut-based composites achieved absorption comparable to polyurethane, while bentonite enhanced reflection and durability [11]. Currently, there is a paucity of study about the hybridization of agricultural biomass with ceramic particles. Prior studies have concentrated on single fibers; however, there has been minimal investigation into the collective properties of these two fiber types. This research presents an innovative approach to enhance epoxy composites hybridized with $ZrO_2$ nanoparticles through the use of a blend of jackfruit peel fibers and palmyra palm fruit waste, both sourced from agricultural biomass. This work aims to address a knowledge gap by examining the physical and mechanical properties of composites. The research findings will enhance bio-based composites utilized in several automotive applications, including door panels, seat backs, and interior panels.

## 2 Materials and Methods

### 2.1 Materials

The naturally occurring fibrous material from the palmyra palm fruit is cylindrical in form. The Arecaceae family of plants, from which it is derived, is adapted to flourish in humid regions. The chemical compositions of Palmyra palm fruit and jackfruit peel fibers are presented in Table 1. Palmyra palm and jackfruit peels were collected from various places in and around Coimbatore, Tamilnadu, India. Zirconium dioxide ($ZrO_2$) powder was utilized as a filler to enhance the strength of the composite. Matrics Enterprises, in Nagercoil, Tamil Nadu, India, provided the 50 nm $ZrO_2$ nano particles. Characteristics including density (3.98 g/cc), tensile strength (416 MPa), and coefficient of thermal expansion ($7.4\times10^{-6}$/ºC) are all evident. The matrix material for this investigation was obtained from M/s Covai Seenu Traders in Coimbatore, Tamil Nadu, India, comprising LY556 epoxy resin with a density of 1.13 g/km$^3$ and HY951 hardner with density of 0.98 g/cm$^3$.

**Table 1.** Chemical composition of the natural fibers

| Sl. No. | Chemical constituent | Palmyra palm fruit fiber (%) | Jackfruit peel fiber (%) |
|---|---|---|---|
| 1 | Cellulose | 58.56 | ~20.08 |
| 2 | Hemicellulose | 16.29 | ~24.04 |
| 3 | Lignin | 12.87 | ~1.85 |
| 4 | Residue | 2.38 | ~7.01 |
| 5 | Wax, Moisture, Pectin etc. | Pectin 1.33 % Fat/Wax 0.63 % | Pectin ~7.52 %, wax~5.218 %, Moisture ~12.98 % |

### 2.2 Preparation of Palmyra Palm Fruit Fiber-Waste and Jackfruit Peel Fibers

Initially, the collected palmyra palm and jackfruit peels were thoroughly washed with normal water to remove dust and skin of the jackfruit peels.

A crucial aspect of fiber production is the alkali treatment to eliminate impurities and enhance adhesion to the resin. The fibers were soaked in 10% NaOH solution at room temperature for one hour. To enhance the fiber's adhesion to the matrix, it is advantageous to eliminate surface contaminants from plant fibers. This is achieved by improving the mechanical bonding and interlocking responses. Subsequently, there were separate washing procedures for the processed palmyra palm fruit fibers and the discarded jackfruit peel fibers. Subsequent to getting cleaned in fresh water, they were rinsed once more in distilled water. The objective of this method was to completely eliminate any residual sodium hydroxide (NaOH) present on the fibers' surface. Subsequently, the treated fibers were allowed to air dry for 24 hours at 60℃. Hybrid fibers composed of palmyra palm fruit and discarded jackfruit (*Artocarpus heterophyllus*) peel were produced by meticulously rinsing both fiber types with water. An alkalization treatment is essential to eliminate impurities and improve the fiber surface's adhesion to the resin. The fibers were subsequently immersed in a 5% NaOH solution at ambient temperature for sixty minutes. The removal of contaminants from plant fibers enhances mechanical interlocking and bonding interactions with the matrix. Subsequently, a mixture of fresh water and distilled water was employed to meticulously cleanse the treated palmyra palm fruit fibers and the discarded jackfruit peel fibers. The residual NaOH content was effectively eliminated by this method. The subsequent phase was drying the fibers in ambient air for 24 hours.

### 2.3 Preparation of Composites

The composite panels utilized in this research were fabricated with the conventional open-mold hand layup technique. Fibers and resin are manually arranged in a mold by the hand layup procedure also known as the wet layup technique. This technology has grown prevalent in composite production due to its user-friendliness, affordability, and capacity to produce intricate designs. This technology enables the creation of composites that are both robust and uniform by meticulously regulating the orientation of the fibers and the distribution of the resin. Table 2 indicates that the composites were fabricated using various combinations of hybrid fibers derived from palmyra palm fruit fibers and jackfruit peel (20 wt. %, 25 wt. %, and 30 wt. %) alongside differing quantities of $ZrO_2$ nano filler (2.5 wt. %, 5 wt. %, and 7.5 wt. %). A hybrid fiber-reinforced composite material is utilized to produce $ZrO_2$ nano fillers, as seen in Fig. 1. At ambient temperature, the particles are meticulously blended with the epoxy resin. The last step is to meticulously swirl the mixture to ensure uniform distribution of the particles within the base matrix. The subsequent stage involves adhering to the manufacturer's guidelines and incorporating the HY951 hardener into the LY556 epoxy resin at a weight ratio of 10:1. The conventional hand layup technique is employed to fabricate composite materials in an open mold measuring 270×210×3 $mm^3$. To facilitate the removal of the composite panels, the release coating was initially applied to the mold. Table 2 presents the ratios employed to combine the fibers of palmyra palm fruit with those of discarded jackfruit skin. The $ZrO_2$-dispersed epoxy was uniformly applied to the fibers using a brush after they were arranged randomly within the mold. The subsequent stage involved employing a hand roller to evenly distribute the matrix mixture within the mold. After 24 hours, the mold was subjected to approximately 25 kg of weight to eliminate any surplus resin and air bubbles. Specimens were fabricated and tested per ASTM standards.

**Table 2.** Composition of the composite samples

| Sl. No. | Designation | Compositions | | | | |
|---|---|---|---|---|---|---|
| | | Palmyra palm fruit fiber (wt. %) | Jackfruit peel fiber (wt. %) | Total fiber (wt. %) | $ZrO_2$ (wt. %) | Epoxy (wt. %) |
| 1 | CS1 | 10 | 10 | 20 | 0 | 80 |
| 2 | CS2 | 12.5 | 12.5 | 25 | 0 | 75 |
| 3 | CS3 | 15 | 15 | 30 | 0 | 70 |
| 4 | CS4 | 10 | 10 | 20 | 2.5 | 77.5 |
| 5 | CS5 | 12.5 | 12.5 | 25 | 2.5 | 72.5 |
| 6 | CS6 | 15 | 15 | 30 | 2.5 | 67.5 |
| 7 | CS7 | 10 | 10 | 20 | 5 | 75 |
| 8 | CS8 | 12.5 | 12.5 | 25 | 5 | 70 |
| 9 | CS9 | 15 | 15 | 30 | 5 | 65 |
| 10 | CS10 | 10 | 10 | 20 | 7.5 | 72.5 |
| 11 | CS11 | 12.5 | 12.5 | 25 | 7.5 | 67.5 |
| 12 | CS12 | 15 | 15 | 30 | 7.5 | 62.5 |

## 2.4 Characterization using XRD Analysis

XRD analysis was conducted to examine the chemical composition of the treated palmyra palm fruit, jackfruit peel fibers, and $ZrO_2$ fillers. The Bruker XRD apparatus (Model: D8 advance) was employed for XRD analysis, with a Bragg's range (2θ) of 10˚ to 80˚, a voltage of 30 mV, and a current of 3 mA. The X-ray source was CuKα radiation with a wavelength of 1.54 Å.

## 2.5 Density Test

The weight fraction is utilized to get the theoretical density ($\rho_c$) of the composites by using Equation (1). The water immersion procedure was conducted in line with the ASTM D792 standard in this investigation. The density ($\rho_E$) of the composites were determined by weighing balance equipped with both a water column and an air column. To get the volume void fraction ($V_{voids}$) of the composite laminates, Equation (2) was utilized.

$$\rho_c = \frac{1}{\frac{W_f}{\rho_f}+\frac{W_p}{\rho_p}+\frac{W_m}{\rho_m}} \quad (1)$$

The weight fractions of the fiber, matrix, and particle are denoted as $W_f$, $W_m$, and $W_p$, respectively, while their densities are represented by $\rho_f$, $\rho_m$, and $\rho_p$.

$$V_{voids} = \frac{\rho_c - \rho_E}{\rho_c} \quad (2)$$

The volume proportion of voids, theoretical density of the composite, and experimental density of the composite are denoted by $\rho_a$ and $\rho_c$, respectively. Composite specimens were subjected to tensile, flexural, impact, and interlaminar shear strength testing using a Kalpak computerized universal testing machine (Model KIC-2-1000C) at a crosshead speed of 2 mm/min.

The specimens were prepared in accordance with ASTM criteria. The following standards were specifically followed: ASTM D3039 for tensile testing, ASTM D790 for flexural testing, ASTM D256 for impact testing, and ASTM D2344 for interlaminar shear strength (ILSS) testing. The specimens utilized in these experiments possessed the following dimensions: 127×12.7×4 mm for the tensile testing, 64×13×4 mm for the flexural testing, and 48×12×3 mm for the ILSS. The impact testing machine is utilized for testing V-notched specimens for impact. The hybrid composite samples underwent testing with a Shore-D durometer at a 50 N load for a duration of 5 seconds to determine their hardness. Five specimens were selected for each composite category, with the mean value of the results representing the specific feature associated with each composite. The fractured surface morphology of the composites was analyzed using a Carl Zeiss SEM. Prior to the SEM analysis, the specimens were subjected to gold sputtering at a continuous current of 30 mA for a duration of 30 seconds. Fig. 1(a) to Fig. 1(d) depicts the images of Universal Testing Machine, specimens for tensile, flexural, and impact test correspondingly.

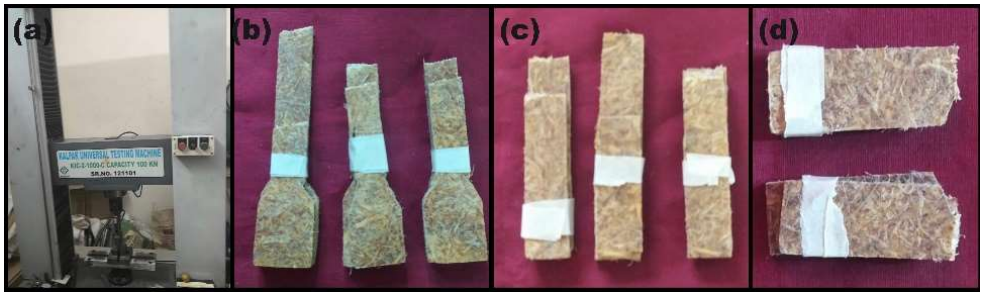


**Fig. 1.** (a) Universal Testing Machine, Specimen for (b) Tensile, (c) Flexural, and (d) Impact test.

## 3 Results and Discussions

### 3.1 X-Ray Diffraction Analysis

Fig. 2(a) to Fig. 2(c) shows the spectra of palmyra palm fruit fiber, jackfruit peel fiber (JPF), and $ZrO_2$ nano particles. The diffraction profile of palmyra palm fruit fiber exhibited distinct crystalline peaks at $2\theta$ = 16°, 22°, and 34°, with the most intense reflection observed at 22°, corresponding to the characteristic cellulose crystalline plane. In contrast, JPF showed peaks at $2\theta$ = 15°, 18°, 22°, and 34°, where the dominant reflection at 18° indicated its relatively lower crystallinity. The XRD pattern of $ZrO_2$ revealed sharp and intense peaks at $2\theta$ = 28°, 32°, 35°, 50°, and 60°, with the maximum intensity observed at 28°, confirming its highly crystalline structure. These findings suggest that the incorporation of high-crystalline $ZrO_2$ nano fillers, in conjunction with palmyra palm fruit fiber, enhances the overall crystallinity of the hybrid composites, thereby improving their mechanical strength and thermal stability.

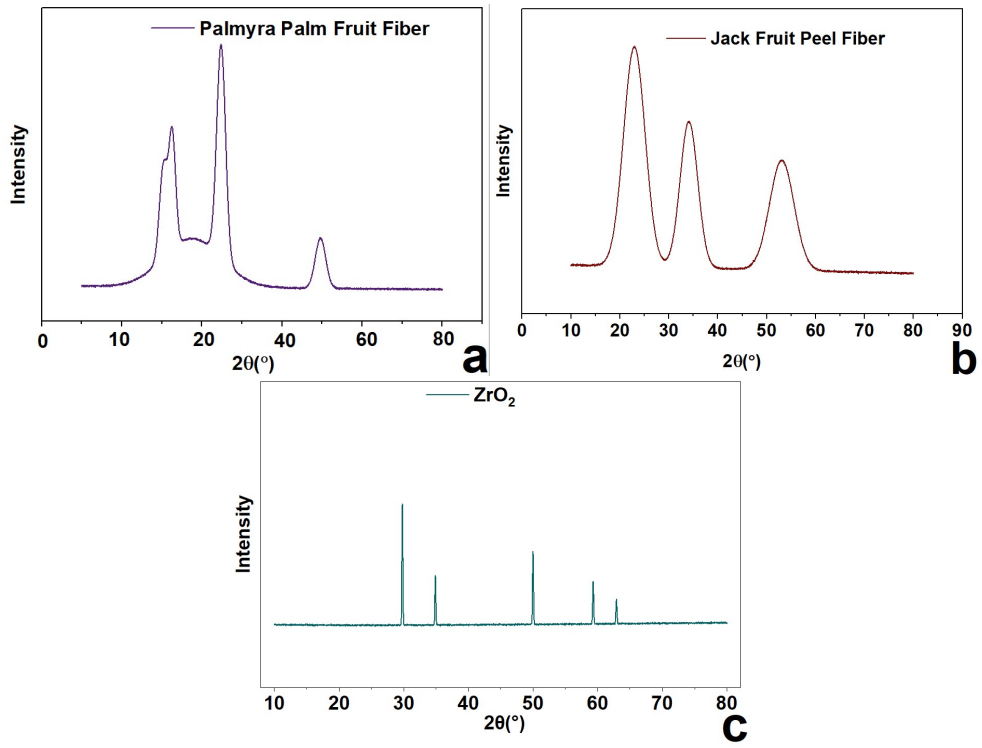


**Fig. 2.** XRD peaks of (a) Palmyra palm fruit fiber, (b) Jack fruit peel fiber, and (c) $ZrO_2$

### 3.2 Density and Void Content

The densities of composites were determined and compared with corresponding theoretical value. Researchers discovered that, the observed density values varied in the presence of voids inside the composites. Fig. 3(a) illustrates the influence of fiber and filler content on the voids inside the composite laminates. The subsequent step involved quantifying and comparing the densities of the composites to their respective theoretical densities. It was observed that voids influenced the density values derived from the composites. Fig. 3(a) illustrates that voids were minimal (~1.5%) in the unfilled composite at 20 wt. % fiber loading and maximal (~7%) in the 7.5 wt. % filler composite at 30 wt. % loading. Void content often escalated with the augmentation of both fiber fraction and filler incorporation, attributable to inadequate resin wetting at elevated loadings. The incorporation of $ZrO_2$ nano filler in the matrix at 2.5, 5, and 7.5 wt. % augmented the formation of voids in the composite. This occurs because to the entrapment of air between the matrix and filler during their amalgamation. Insufficient wetting of the fibers may result in voids inside laminates. The mechanical properties of the composite material influenced by presence of voids. Superior composites exhibit fewer voids, serving as a significant quality indication. Void generation in composite laminates is an inherent result of the hand-lay-up manufacturing technique.

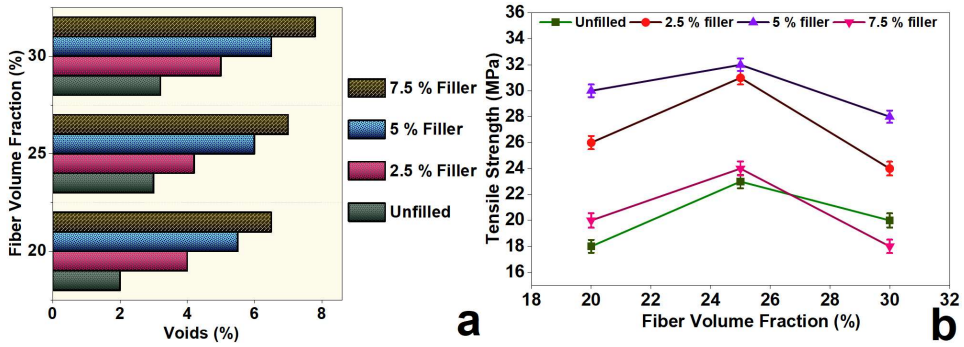


**Fig. 3.** (a) Variation of void content, and (b) tensile strength for various composite configurations.

### 3.3 Tensile Strength

The proportion of fibers and their tensile strength (TS) determine the strength of the composite materials. Fig. 3(b) illustrates the variation in tensile strength properties of the composite materials concerning the filler contents. A fiber composition of up to 25 wt. % increases the tensile strength. However, beyond this threshold, the tensile strength diminishes as the fiber concentration increases. Composites can enhance their load-bearing capacity by up to 25 wt. %, evidenced by the significant increase in strength. This may be attributed to the epoxy resin transfers that facilitate stress distribution across the composites. This results in enhanced strength of the composites. The composite tensile strengths increased linearly with the fiber content, reaching up to 25 wt. %. Prior research indicated that palmyra palm fruit fiber reinforced hybrid polymer composites demonstrated a tensile strength of about 53.62 MPa while the greatest TS of current hybrid composites reached 32 MPa. Nonetheless, the TS reduced with additional increments in fiber content [12]. The observed decrease in tensile strength at 25 wt. % fiber loading attributed to the inadequate interfacial bond between the matrix and the fibers. Chemical treatment of hybrid fibers derived from palmyra palm fruit and jackfruit peel fiber significantly enhanced the TS of fiber-reinforced composites. XRD analysis indicates that surface-modified fibers enhance crystallinity, hence improving stress transfer from the matrix to the reinforcement by facilitating greater interlocking between the matrix and fiber. Fig. 3(b) illustrates that the TS of hybrid composites escalated with fiber loading up to 25 wt. %, then declining at 30 wt. %. The unfilled composite exhibited a minimum tensile strength of around 18 MPa at 20 wt. % fiber loading, whereas the 5 wt. % filler composites attained a maximum tensile strength of roughly 34 MPa at 25 wt. % fiber loading. The decline at elevated loading (about 22 MPa at 30 wt. % fiber with 7.5 wt. % filler) is ascribed to fiber aggregation and inadequate wettability. In general, filled composites regularly surpassed empty composites, validating the beneficial impact of filler incorporation on tensile performance. The TS of the composite materials increases with the addition of the filler, reaching a concentration of 5 wt. %, as indicated by the plots. The improved tensile strength of the composites results from the uniform distribution of the filler within the material. The TS of composites diminishes as the content of filler increases, especially at 25 wt. %. A potential source of the issue may be inadequate adhesion between the epoxy matrix and the filler at the interface. The larger quantity of filler resulted in mixing issues, preventing uniform distribution throughout the composite materials. In another study, Palm fruit fiber reinforced epoxy composites were enhanced with boron carbide nanoparticles. At 4 wt. % $B_4C$, tensile (41.73 MPa), flexural (43.29 MPa), and impact (5.6 kJ/m²) strengths peaked, along with improved hardness [13].

### 3.4 Tensile Modulus

Fig. 4(a) illustrates the impact of incorporating fibers and fillers into the composite laminates on their tensile modulus. The elevation of fiber concentration is positively connected with the modulus of composite materials. As the fiber content increases, the composite exhibits greater brittleness and the stress-strain curves get steeper. Insufficient interfacial bonding prevents stress transmission from the fiber to the matrix, resulting in the formation of a partially detached micro-space. A rise in fiber content was favorably associated with the stiffness of the composites. The level of obstruction similarly escalated in accordance with the fiber content. Fig. 4(a) illustrates that the tensile modulus was minimal (~650 MPa) for the unfilled composite at 20 wt. % fiber loading and maximal (~1050 MPa) for the 5wt. % filler composite at 25 wt. % fiber loading. Filled composites consistently surpassed empty variants, with 25 wt. % fiber and 5 wt. % filler yielding the optimal rigidity. As the filler fraction increases, the tensile modulus of n$ZrO_2$-filled hybrid composites increases. The tensile modulus of hybrid composites increases with the addition of filler. The $ZrO_2$ nanoparticles are often hard and brittle. Thus, as the filler loadings increase, the elongation of the composite material will diminish. An increased tensile modulus for hybrid composites is an additional advantage of this phenomenon. In previous study, palm fiber-reinforced PLA composites with bran filler were studied for thermal and dynamic stability. The 15 g filler sample showed best performance, with 25 MPa fatigue strength and high modulus (2400 MPa).

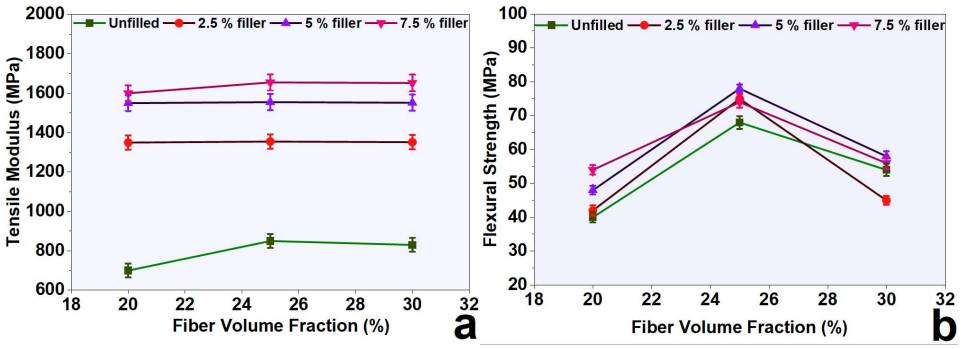


**Fig. 4.** Variation of (a) tensile modulus, and (b) flexural strength for various composite configurations.

### 3.5 Flexural Strength

Fig. 4(b) illustrates the impact of varying filler loadings on the flexural strength of composites, dependent on fiber and filler concentration. The flexural strength of the composites exhibited a comparable pattern; it initially increased, reached a maximum at 25 wt. % fiber, and thereafter declined. A reduction in flexural strength exceeding 25 wt. % relative to fiber content. The reduction in flexural strength with raising fiber content suggests insufficient bonding within the fiber matrix, leading to the formation of micro-cracks at the interface. The diminished flexural strength at elevated fiber concentrations results from inadequate adhesion between the fiber and matrix. The findings regarding tensile strength align with the observed relationship between the increased filler quantity and improved flexural strength. Composites containing 5 wt. % of $ZrO_2$ nano filler exhibited superior flexural strength compared to their unfilled equivalents.

Fig. 4(b) illustrates that the flexural strength was minimal (~32 MPa) for the unfilled composite at 20 wt. % fiber loading and maximal (~92 MPa) for the 5 wt. % filler composites at 25 wt. % fiber loading. Beyond 25 wt. %, the strength diminished; yet, filled composites generally outperformed empty composites. Composites containing additional fillers have enhanced flexural strengths due to their increased resistance to fracture initiation and propagation. This boost becomes evident at filler loadings of up to 5 wt. %. In another study, optimal composition of 40% Borassus fruit fiber and 40 % cigarette butt fiber, with 5% eggshell powder as filler achieved tensile 53.62 MPa, flexural 38.67 MPa, and impact 37.78 J/m [14]. Various mechanisms, including as shearing, tensile, and compression, are employed in flexural testing. Insufficient adhesion between layers results in a decrease in shear strength as filler content increases.

### 3.6 Impact Strength

Fig. 5(a) illustrates the influence of filler loading on the impact strength of hybrid composites. The hybrid fiber composites composed of palmyra palm fruit and jackfruit peel fibers exhibited remarkable impact resistance. An elevation in fiber content to 25% by weight correlates with a proportional enhancement in impact strength, which demonstrates the relationship between the two variables. Fig. 5(a) illustrates that the impact strength was minimal (~0.8 J) for the unfilled composite at 20 wt. % fiber loading and maximal (~2.1 J) for the 2.5 wt. % filler composite at 25 wt. % fiber loading. Exceeding 25 wt. %, the strength diminished, however filled composites typically surpassed unfilled counterparts.

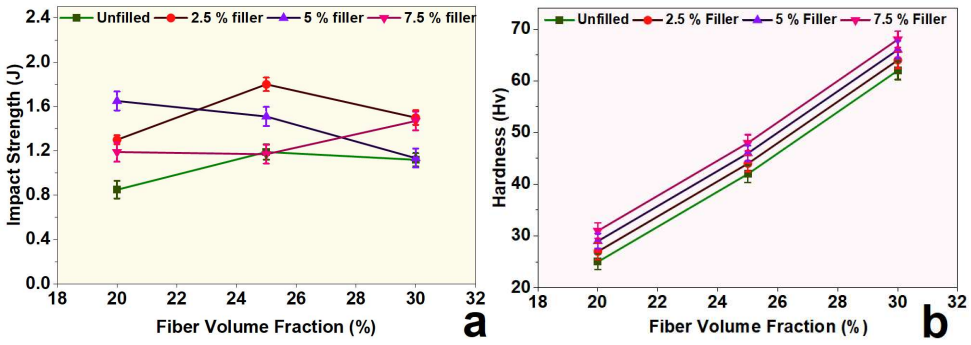


**Fig. 5.** Variation in (a) impact strength, and (b) hardness for various composite configurations.

The robust bond between the matrix and fibers at the interface accounts for this enhancement. The impact strength is enhanced as this bonding facilitates energy absorption and prevents the initiation of cracks. Despite appearing contradictory, impact strength diminishes as fiber content escalates. Composites may fail owing to fiber-matrix debonding, matrix fracture, or fiber pull-out when impacted. All of these processes collaborate to induce failure in composites under impact loads. Factors, including as the dimensions and the degree of human interference and type of filler material, may influence the impact strength and require meticulous consideration. Additional research is required to investigate these factors and ascertain their influence on the impact strength of hybrid composites.

### 3.7 Hardness

The hardness of a composite sample was characterized by its resistance to localized plastic deformation. Fig. 5(b) illustrates the association between composite hardness values and hybrid composite percentages with varying filler percentage. The image distinctly illustrates that the quantity of filler and fiber content is correlated with the hardness of the hybrid compounds. Fig. 5(b) illustrates that hardness escalated with fiber loading from 20 wt. % to 30 wt. %, exhibiting a minimum value (~22 HV) for the unfilled composite at 20 wt. % and a maximum value (~68 HV) for the 15 wt. % filler composites at 30 wt. %. Filled composites consistently demonstrated superior hardness compared to unfilled composites. Composites are recognized for their hardness due to the robust bonds formed between the polymer matrix and the filler. The material's indentation resistance is enhanced by these links. The utilization of filler has resulted in an increased hardness value. The enhancement of composite penetration resistance is attributed to the uniform distribution of filler content and the decreased interparticle distance inside the matrix. The interlocking mechanism likely accounts for the observed increase in hardness following the incorporation of $ZrO_2$ nano filler into the polymer matrix.

### 3.8 Inter-Laminar Shear Strength (ILSS)

A method to determine resilience to shear stress at the interface of two adjacent laminate is by assessing their interlaminar shear strength (ILSS). The ILSS values of hybrid composites treated and filled with $ZrO_2$ nano filler are presented in Fig. 6. Incorporating 2.5-7.5 wt. % of $ZrO_2$ nano filler into composites enhances their interlaminar shear strength (ILSS) value. The impact of augmenting adhesion at the matrix-filler interface is pertinent in this context. Key properties that enhance ILSS features comprise robust interfacial bonding between the matrix and the filler, facilitating load transfer between the two, and the capacity of the filler materials to convey their own load to the matrix. Composites with increased fiber content have elevated ILSS values. It demonstrates that ILSS values increase with fiber content up to 25 wt. %. Fig. 6 illustrates that the interlaminar shear strength was minimal (~57 MPa) for the unfilled composite at 20 wt. % fiber loading and maximal (~84 MPa) for the 10 wt. % filler composites at 25 wt. % loading. Strength diminished by 30 wt. %, although filled composites routinely surpassed unfilled counterparts. With the increase in $ZrO_2$ nano filler content, a positive correlation was noted between the ILSS value and the filler content, indicating a progressive rise in the ILSS value. The presence of filler material adhering to the fiber ends is likely accountable for the observed increase in this phenomenon. The barrier function of these fillers efficiently prevents shear forces from transmitting through the material. The ILSS value of composites decreases as the fiber content increases from 25 wt. % to 30 wt. %. The existence of voids at the composite interface, which develop and expand over time could be the reason for this phenomenon.

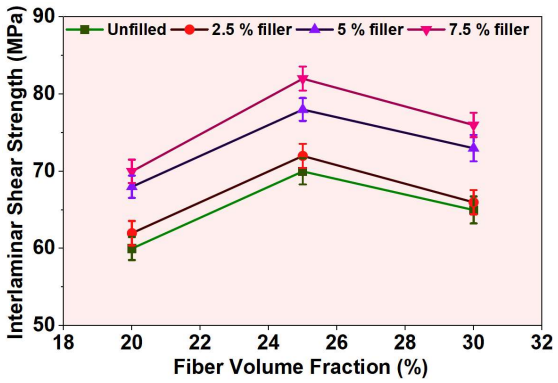


**Fig. 6.** Variation of ILSS for various composite configurations.

### 3.9 Failure Surface Morphology

The hybrid composite specimens exhibit fracture surface morphology under tensile load in Fig. 7(a) and under flexural stress in Fig. 7(b). The fragile nature of crack initiation and propagation under tensile stress is demonstrated by the clear fracture propagation and river pattern in Fig. 7(a). River marks indicate that stress is efficiently transmitted from fiber to matrix by highlighting certain stress concentration areas and the path of fracture propagation inside the matrix. The increased tensile strength resulted directly from the robust adhesion, which inhibited premature debonding. Fig. 7(b) illustrates the fracture morphology under flexural pressure, revealing fiber breakage and voids resulting from fiber pull-out. The existence of these voids indicates that the bending process resulted in localized debonding and stress concentration. The transverse loading condition prompted fiber rupture, indicating the limited capacity of palmyra palm fruit fiber to independently withstand bending stresses, despite the matrix-fiber adhesion being sufficiently robust to reduce extensive fiber pull-out. Nonetheless, fillers significantly aided in redistributing stress, hence enhancing the overall flexural performance. The confirmation that the hybrid composite effectively manages flexural loads with little pull-out and fiber fracture substantiates that the combination of 25 wt. % fiber and 5 wt. % $ZrO_2$ enhances mechanical strength for semi-structural applications. SEM confirmed stronger fiber–matrix interfacial bonding in the optimized hybrid system [15].

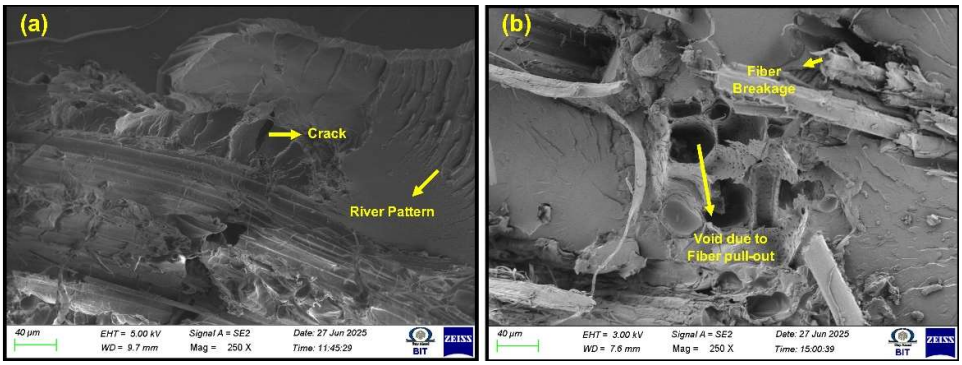


**Fig. 7.** Failure surface morphology of CS8 specimen under (a) tensile load, (b) flexural load.

## 4 Conclusions

This study examines the hand lay-up technique for fabricating jackfruit peel hybrid fiber reinforced epoxy composites, both with and without $ZrO_2$ nano filler material. Experiments were performed to assess the mechanical and physical characteristics of the hybrid composites. An increase in the void content of the pre-treated hybrid composites is observed when the fiber and filler content rise. With an increase in the percentage of $ZrO_2$ nano filler in hybrid composite materials, the mechanical properties, including flexural strength (78 MPa), tensile strength (32 MPa), impact strength (1.8 J/mm²), and interlaminar shear strength (ILSS) (82 MPa), exhibit enhancement. The strength was enhanced since this filler facilitated the transmission of stress from the continuous matrix phase to the dispersed fiber phase. Incorporating 5 wt. % of $ZrO_2$ nano filler into the composite material enhanced its mechanical strength. The $ZrO_2$ nano filler significantly influences the density, tensile modulus (1555 MPa), and hardness (64) in composite materials. Moreover, the mechanical properties of composite materials exhibited enhancement when comprising 25 wt. % fiber by weight. Composites have an enhancement in tensile modulus with elevated fiber and filler content. Composites containing up to 25 wt. % exhibit enhanced interlaminar shear strength (ILSS). The ILSS value will increase in hybrid composites containing a filler concentration of 2.5-7.5 wt. % of $ZrO_2$.The failure surface morphology of the hybrid composites indicates that a composite with 25 wt. % fiber and 7.5 wt. % of $ZrO_2$ enhanced the adhesion at the interface between the matrix and the filler. This study yields significant insights into the ILSS, hardness, and impact strength of epoxy composites supplemented with hybrid fibers derived from jackfruit peel fibers. Nonetheless, it is essential to acknowledge that this research possesses specific limitations. The research concentrated on a particular spectrum of fiber and filler concentrations. However, further research is required to ascertain the impacts of various ratios and combinations. Further constraints encompass an absence of research about the composites' long-term durability and the implications of aging. Future experiments may examine how additional variables, such as humidity and temperature, influence the mechanical properties of the composites.

## References

1. R. Saravanan, R. Anand, C. Boopathi, L. Ganesh Babu, A. Yasminebegum, G. Ravivarman, R. Girimurugan, Mechanical Properties of Polyethylene/Hemp/Lignin Hybridized Composites. International Journal of Vehicle Structures & Systems. **16,** 738 (2024).
2. R. Girimurugan, P. Rajasekaran, Ganesh Babu Loganathan, A. G. Gandhi, Harishchander Anandaram, R. Edwin Josep, Influence of E-Glass Fiber Addition on Mechanical Properties of Jute Fiber Reinforced Hybrid Composites. International Journal of Vehicle Structures & Systems. **16,** 723 (2024).
3. A. Rahman, S. M. A. Nipu, M. S. Alam, S. S. Alam, M. T. Ahmed, A. A. Shantona, M. Moon, Extraction of Cellulosic Compound from Jackfruit Peel Waste and Characterization of PVA Cellulose Composite as Biodegradable Film. Journal of Nanomaterials. **2024**, 5052750 (2024). https://doi.org/10.1155/2024/5052750
4. B. S. Lazarus, V. Leung, R. K. Luu, M. T. Wong, S. Ruiz-Pérez, W. T. Barbosa, W. B. A. Bezerra, J. D. V. Viana Barbosa, M. A. Meyers, Jackfruit: Composition, structure, and progressive collapsibility in the largest fruit on the Earth for impact resistance. Acta Biomaterialia. **166**, 430 (2023). https://doi.org/10.1016/j.actbio.2023.04.040

5. P. Senthamaraikannan, N. P. Sunesh, D. Divya, S. Sumesh, I. Indran, S. Siengchin, Extraction and characterization of biomass microcrystalline cellulose from Terminalia catappa leaves for food packaging applications. Biomass Conversion and Biorefinery. **15**, 17029 (2025). https://doi.org/10.1007/s13399-024-06328-0
6. V. P. Suresh Kumar, S. Seenivasan, G. B. Loganathan, P. Jayanthi, R. Girimurugan, S. Hasane Ahammad, Enhancing Mechanical Properties of PLA/Kevlar Fiber Composites with $ZrO_2$ Nanorod Interface Modification for High-Performance Applications. Advances in Science, Technology & Innovation (2024). https://doi.org/10.1007/978-3-031-63909-8_28
7. D. K. Singh, R. K. Verma, Production of zirconia modified ultra-high molecular weight polyethylene polymeric bio-nanocomposites: evaluation of wear mechanisms and fracture behavior. Journal of Polymer Engineering.**17**, 8301 (2025). https://doi.org/10.1080/00405000.2025.2499339
8. A. Hadi, N. S. Radhi, Structure and Mechanical Properties of (PMMA–$ZrO_2$–Ag) Nanocomposites for Medical Applications. Nanosystems: Physics, Chemistry, Mathematics. **20**, 809 (2022). https://doi.org/10.15407/nnn.20.03.809
9. C. Srikanth, G. M. Madhu, S. J. Kashyap, Enhanced structural, thermal, mechanical and electrical properties of nano ZTA/epoxy composites. AIMS Materials Science. **9**, 214 (2022). https://doi.org/10.3934/matersci.2022013
10. S. S. D. Kumar, R. Resselian, D. A. Dev Anand, Y. Thooyavan, J. S. Joseph Selvi, Optimization of fiber content, length and its effect on overall properties of Licuala grandis leaf stalk fiber/polyester reinforced bio-composites. Journal of Polymer Science. **62**, 5265 (2024). https://doi.org/10.1002/pol.20240526
11. M. K. Jha, P. P. Das, V. Pandey, P. Gupta, V. Chaudhary, S. Gupta, Water immersion aging of polymer composites: architectural change of reinforcement, mechanical, and morphological analysis. Biomass Conversion and Biorefinery. **14**, 15769 (2024). https://doi.org/10.1007/s13399-022-03622-7
12. U. Victoria-Martínez, S. Loera-Serna, E. R. Vázquez-Cerón, Acoustic properties of composite materials based on bentonite and coconut or cactus (nopal) fibers. Journal of Composite Materials. **57**, 3173 (2023). https://doi.org/10.1177/00219983231185101
13. M. Sriariyanun, P. Paramasivam, S. Venkatesh, K. Rajeshkumar, V. Vijayananth, Manufacturing and mechanical characterization of alkali-treated Borassus fruit natural fiber with cellulose acetate synthetic fiber reinforced polymer composite: selection of optimum configuration using CRITIC-integrated EDAS soft computing techniques. Waste and Biomass Valorization. **27**, 880 (2025). https://doi.org/10.1007/s10163-024-02142-y
14. T. Raja, Y. Yuvarajan, J. U. Udaya Prakash, V. J. Upadhye, L. Singh, S. Kannan, Sustainable innovations: Mechanical and thermal stability in palm fiber-reinforced boron carbide epoxy composites. Results in Engineering. **24**, 103214 (2024). https://doi.org/10.1016/j.rineng.2024.103214
15. D. Toorchi, E. Tohidlou, H. Khosravi, Enhanced flexural and tribological properties of basalt fiber-epoxy composite using nano-zirconia/graphene oxide hybrid system. Journal of Industrial Textiles. **51**, 3238 (2022). https://doi.org/10.1177/1528083720920573